Assignment 1

Flow for 2D section with camber, thickness and angle of attack

41221 Ship Propulsion and Manoeuvring

by

Franz Hastrup-Nielsen s113399

Coding in cooperation with

Thomas Sørensen s113354
Kristian Ravnborg Nissen s113385

Department of Mechanical Engineering -
Fluid Mechanics, Coastal & Maritime Engineering
Technical University of Denmark

10. October 2014

Contents

1 Introduction

The flow around a 2D section with thickness, camber and angle of attack will be computed for a NACA **a**=0.8 modified foil.

2 Theory and method

The principle of superposition is used for creating this foil. Two scenarios are calculated and at the end superpositioned to give the full solution for a foil with thickness, camber and angle of attack. See figure 2.1.

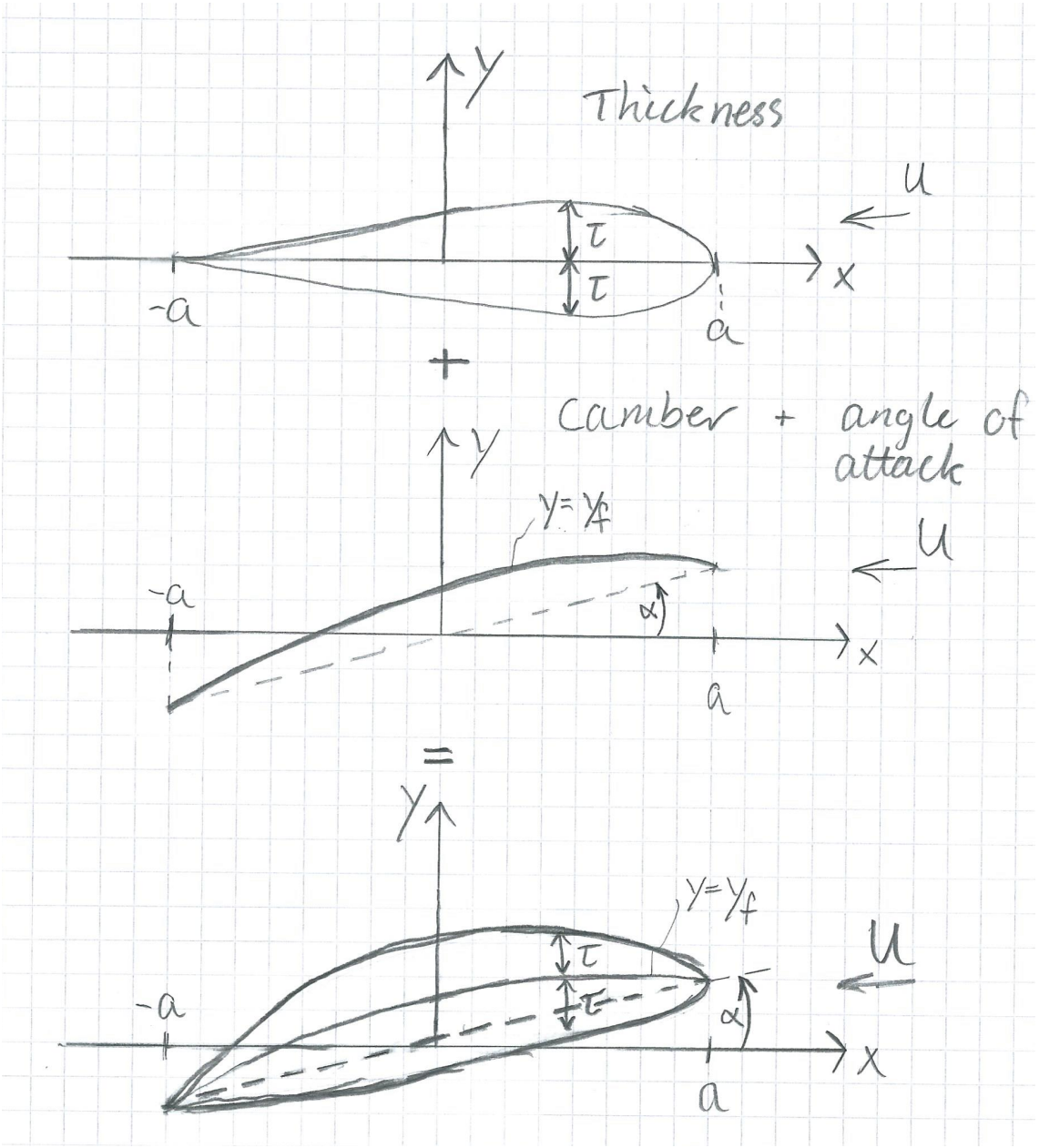

Figure 2.1: Sketch of superposition of thickness and camber with angle of attack.

As seen on the figure the two scenarios are thickness and then camber with angle of attack which in the end will be superpositioned.

2.1 Thickness of a thin 2D section with line source elements

The thickness is created with a dipole, consisting of a source and a sink. This dipole will lead the oncoming flow around the defined edges of the dipole, hence creating the thickness of the foil, see figure 2.2.

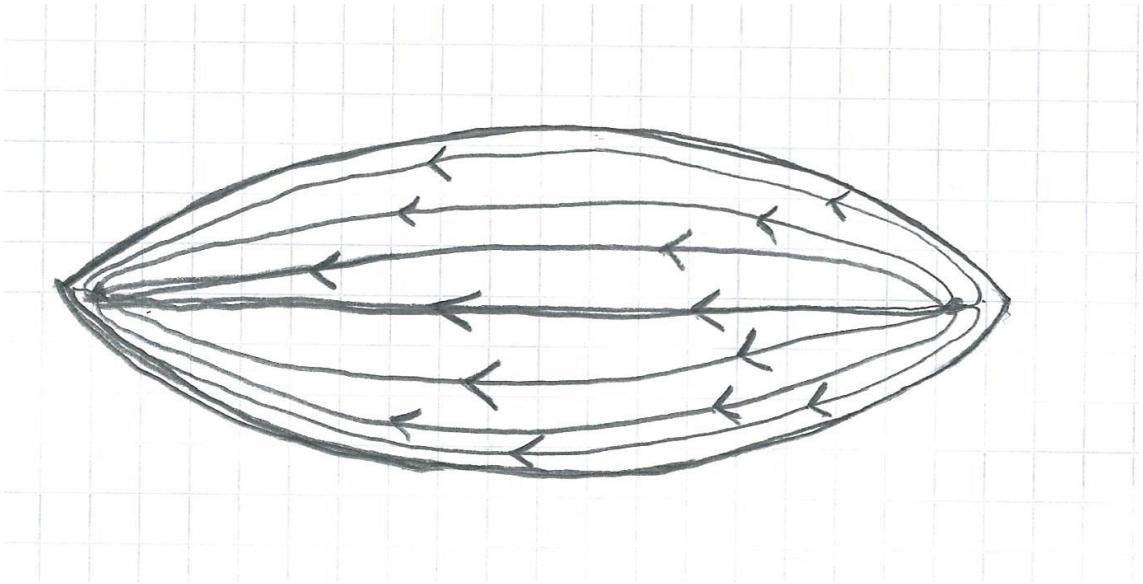

Figure 2.2: Sketch of the dipole used for the thickness.

The thickness from the mean line is defined by τ which can be seen in figure 2.1. The thickness is created with line source elements distributed along the x-axis. The source strength is constant over each element. This means that the solutions of the Laplace's equation are distributed along the line of this finite surface. This is widely used for generating thin symmetrical sections.
The thickness used for this project is choosen as NACA 65-006 Basic Thickness Form with $\frac{t}{c} = 0.06$. The thickness form is plotted and a 6th degree polynomium is created to fit the thickness line, see figure 2.3. The polynomium does not completely fit the NACA thickness at the trailing and leading edge. Within the Matlab script both TE and LE is set to have a thickness of 0, while the rest of the thickness is defined by the polynomium.

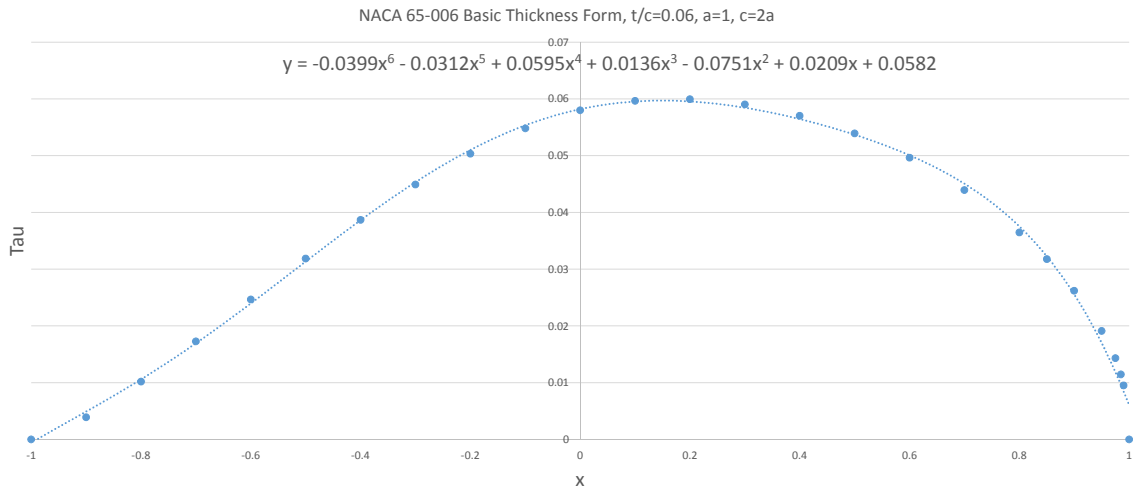

Figure 2.3: The NACA 65-006 thickness and the fitted polynomium used for this task. Both endpoints are set to 0 within the script.

Making the thickness a polynomium has its benefits. It is only dependant on the x-value which means that instead of using the predefined x-values given from NACA it is now possible to use as many x-values as wished. This greatly increases the accuracy of the result.
To compute the solution of the thickness equation (4.15)[1] for the potential is used. The x-values and y-values used for defining the thickness are now defined as:

$$x = x', y = y' \tag{2.1}$$

$$\phi(x,y) = \frac{-U}{\pi} \int_0^{\frac{f}{c}} \int_{-a}^{a} \frac{\partial \tau}{\partial x'} ln\sqrt{(x-x')^2 + (y-y')^2}\, dx'dy' \tag{2.2}$$

To place the line sources along the x-axis, y' is simply set to 0. $\frac{\partial \tau}{\partial x'}$ is simply computed by integrating the polynomium found in figure 2.3. There is a problem with this potential at the leading edge. The assumption for finding this potential is that the induced velocity u is significantly smaller than the onset velocity U, $u << U$. This is true for most of the foil, but not at the leading edge. At the leading edge there is a stagnation point where u = U, and the theory does not hold here. This will definitely influence the pressure coefficient at the leading edge, as seen in figure 4.10[1].
The velocity distribution used is:

$$u(x,y) = -U \frac{\partial \tau}{\partial x'} \int_0^{\frac{f}{c}} \int_{-a}^{a} \frac{(x-x')}{\pi((x-x')^2 + (y-y')^2)} dx'dy' \tag{2.3}$$

$$v(x,y) = -U \frac{\partial \tau}{\partial x'} \int_0^{\frac{f}{c}} \int_{-a}^{a} \frac{(y-y')}{\pi((x-x')^2 + (y-y')^2)} dx'dy' \tag{2.4}$$

2.2 Camber with angle of attack of a 2D section described by point singularities

As seen in figure 2.1 the camber and angle of attack also needs to be computed. For this the NACA mean line with camber curve **a** = 0.8 (modified) is used. As before

the values from NACA are fitted with a polynomium to increase the accuracy of the solution and again both endpoints are manually set to 0. This can be seen in figure 2.4.

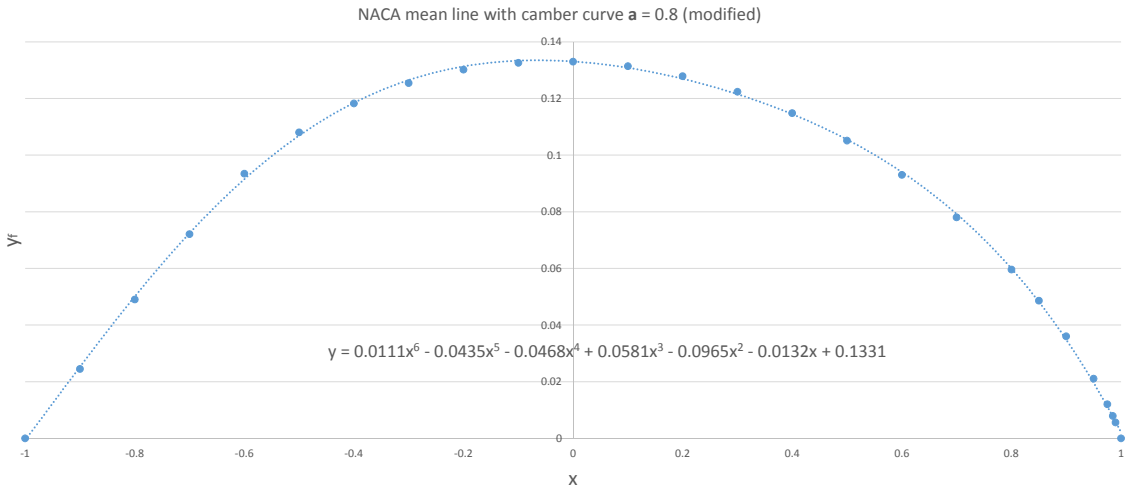

Figure 2.4: The NACA mean line with camber curve **a** = 0.8 (modified) and the fitted polynomium used for this task. Both endpoints are set to 0 within the script.

Then the amount of x-values can be determined by the user hence increasing the accuracy. This solution also needs to take the angle of attack into account. This is done by rotating the entire coordinat system with the given angle of attack. Here x' and y' is the values used to describe the new position of the camber with angle of attack and α is the given angle of attack:

$$x' = cos(\alpha) \cdot x - sin(\alpha) \cdot y_f \tag{2.5}$$

$$y' = sin(\alpha) \cdot x + cos(\alpha) \cdot y_f \tag{2.6}$$

The coordinates are now rotated with the angle of attack.
This 2D section will be described by point singularities, also known as vortexes, placed on the camber itself. These vortexes determines the lift that the camber experiences. The strength of these vortexes will be defined by the kinematic boundary condition.

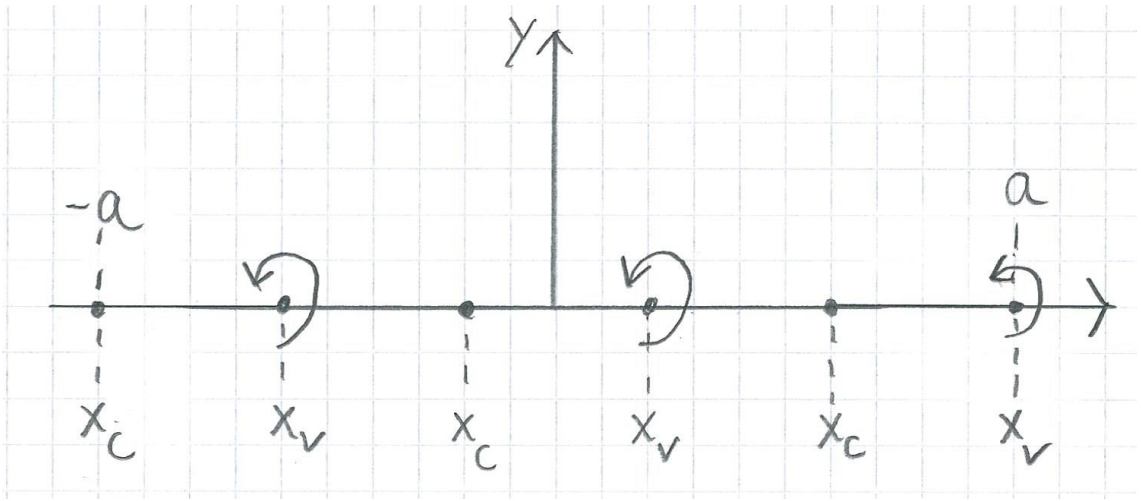

Figure 2.5: Sketch of the point singularities. The leading edge starts with a vortex and the trailing edge has a control point.

In figure 2.5 is a sketch of how the vortexes are placed. The leading edge has a vortex to make sure the camber is well defined. The trailing edge then ends with a control point. The number of vortexes depends on the number of x-values chosen by the user.

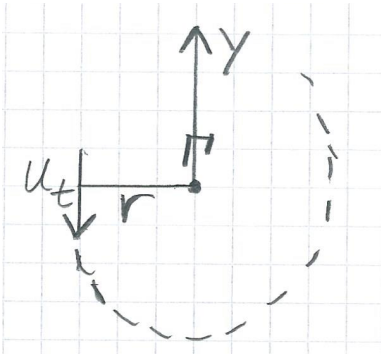

Figure 2.6: A vortex seen from the side.

Figure 2.6 shows the side view of a single vortex. The strength of this vortex is defined as Γ and r is the distance to the outer edge of the vortex, where the tangential velocity, u_t is found.
As already mentioned the strength of the vortexes will be determined from the kinematic boundary condition:

$$\frac{u_t}{U} = \frac{dy(x_c)}{dx} \tag{2.7}$$

This states that the velocity is always tangential to the surface. The tangential velocity is isolated.

$$U \cdot \frac{dy(x_c)}{dx} = u_t = -\frac{1}{2\pi}\frac{\Gamma}{r} = -\frac{1}{2\pi}\frac{\Gamma}{x_c - x_v} \tag{2.8}$$

From this the strength can be determined by setting up a system of equations on the following form:

$$\begin{bmatrix} -\frac{1}{2\pi}\frac{1}{x_{c1}-x_{v1}} & -\frac{1}{2\pi}\frac{1}{x_{c1}-x_{v2}} & \dots \\ -\frac{1}{2\pi}\frac{1}{x_{c2}-x_{v1}} & -\frac{1}{2\pi}\frac{1}{x_{c2}-x_{v2}} & \dots \\ \dots & \dots & \dots \end{bmatrix} \begin{bmatrix} \Gamma_1 \\ \Gamma_2 \\ \dots \end{bmatrix} = \begin{bmatrix} U \cdot \frac{dy(x_{c1})}{dx} \\ U \cdot \frac{dy(x_{c2})}{dx} \\ \dots \end{bmatrix}$$

From this the strength of the vortexes are found. Then the lift of the camber can be computed

$$L = U \cdot \rho \cdot \sum_{i=1}^{n} \Gamma_i \tag{2.9}$$

Furthermore the lift on the flat plate can be found as well

$$L_{flat} = 2 \cdot \pi \cdot \alpha \tag{2.10}$$

The lift coefficient can also be found

$$C_L = 2 \cdot \pi \cdot (\alpha - \alpha_i) + C_{L_i} \tag{2.11}$$

From the vortex strength it is possible to calculate the ΔC_p pressure distribution, but first γ should be found.

$$\gamma = \frac{\Gamma}{dx} \tag{2.12}$$

Where dx denotes the distance between the two control points on each side of the vortex. The velocities at each side of the camber is found

$$u_+ = \frac{-\gamma}{2} \tag{2.13}$$

$$u_- = \frac{\gamma}{2} \tag{2.14}$$

Where the positive sign is on the upper surface. From these velocities the pressure distribution coefficient is found.

$$\Delta C_p = C_{p_-} - C_{p_+} = 2\frac{u_- - u_+}{U} + \frac{u_+^2 - u_-^2}{U^2} \tag{2.15}$$

This coefficient can be compared to the roof-top pressure coefficient distribution for the NACA mean line **a**=0.8 (modified).
The potential for the point singularities is found on page 10[1]. This potential places the point singularities on the x-axis but a more accurate solution is to place them on the camber instead.
The potential with the free stream for the point singularities on the camber:

$$\phi(x,y) = \sum_{i=1}^{n} \frac{\Gamma_i}{2\pi} tan^{-1}\left(\frac{y - y_{v_i}}{x - x_{v_i}}\right) - Ux \tag{2.16}$$

Here x_v and y_v is the vortex coordinates and the potential will be summed for all the Γ's in each (x,y) coordinate.
The potential is differentiated for the velocities.

$$u(x,y) = -\frac{1}{2}\frac{\Gamma(y - y_v)}{(x - x_v)^2\left(1 + \frac{(y-y_v)^2}{(x-x_v)^2}\right)\pi} - U \tag{2.17}$$

$$v(x,y) = \frac{1}{2}\frac{\Gamma}{(x-x_v)\left(1+\frac{(y-y_v)^2}{(x-x_v)^2}\right)\pi} \tag{2.18}$$

Hereby all relevant potentials have been deduced. Hence the superposition can be achieved. This is simply achieved by summing the velocity potentials for both the thickness and camber with angle of attack. The only thing to be aware of is to make sure the free stream is not taken twice for the u-velocities. Before summing the u-velocities the free stream is removed, they are summed and the free stream is inserted again.
Both the dipole and the point singularities are moved onto the camber line. In equation 2.2, this means that y' is no longer 0 but instead equal to the camber lines y-coordinate. This yields a better estimate than placing the singularities on the x-axis

2.3 Cavitation

Assuming that the fluid around the 2D section is water, it could be relevant to look into cavitation.

Cavitation happens when

$$p_{min} < p_v \tag{2.19}$$

This can be rewritten

$$-C_{p,min} = \frac{p_\infty - p_{min}}{\frac{1}{2}\rho U^2} > \frac{p_\infty - p_v}{\frac{1}{2}\rho U^2} = \sigma \tag{2.20}$$

Where p_v is the vapor pressure and σ is the cavitation no. This will not be computed but could be of relevance.

2.4 Drag

The drag coefficient can be estimated for the rough condition, equation 7.5[1].

$$C_D = 0.00850 + 0.0864 \cdot \left(\frac{t}{c}\right)^2 \tag{2.21}$$

2.5 Flaps

After the superposition is done, flaps are added to the script. It is possible to both adjust the length, b, of the flaps and the degrees, β. The implementation of flaps happens by a coordinate change for the length, b, of the chord that the user wants. Then the selected length of the camber measured from the trailing edge undergoes a coordinate change on the following form:

$$x_{flaps} = cos(\beta)\cdot(x-x') - sin(\beta)\cdot(y-y') + x' \tag{2.22}$$

$$y_{flaps} = sin(\beta)\cdot(x-x') + cos(\beta)\cdot(y-y') + y' \tag{2.23}$$

These new coordinates overwrites the existing coordinates within the chosen distance, hence the velocities are calculated around these new coordinates.

3 Results and discussion

The values stated in table 3.1 are tested within the attached script.

Variables	NACA values	Assigned values
Camber, f/c	0.06651	0.030
Thickness, t/c	0.06	0.06
Angle of attack, α°	1.4	1.4

Table 3.1: Overview of the tested values

The result of these tests can be seen below.

3.1 NACA original values

The Matlab script is used with the original NACA values, as seen in table 3.1. The following were used:
a=1
U=1
dx=1.25
$\alpha = 1.4^\circ$
$\beta = 0^\circ$
b = 0

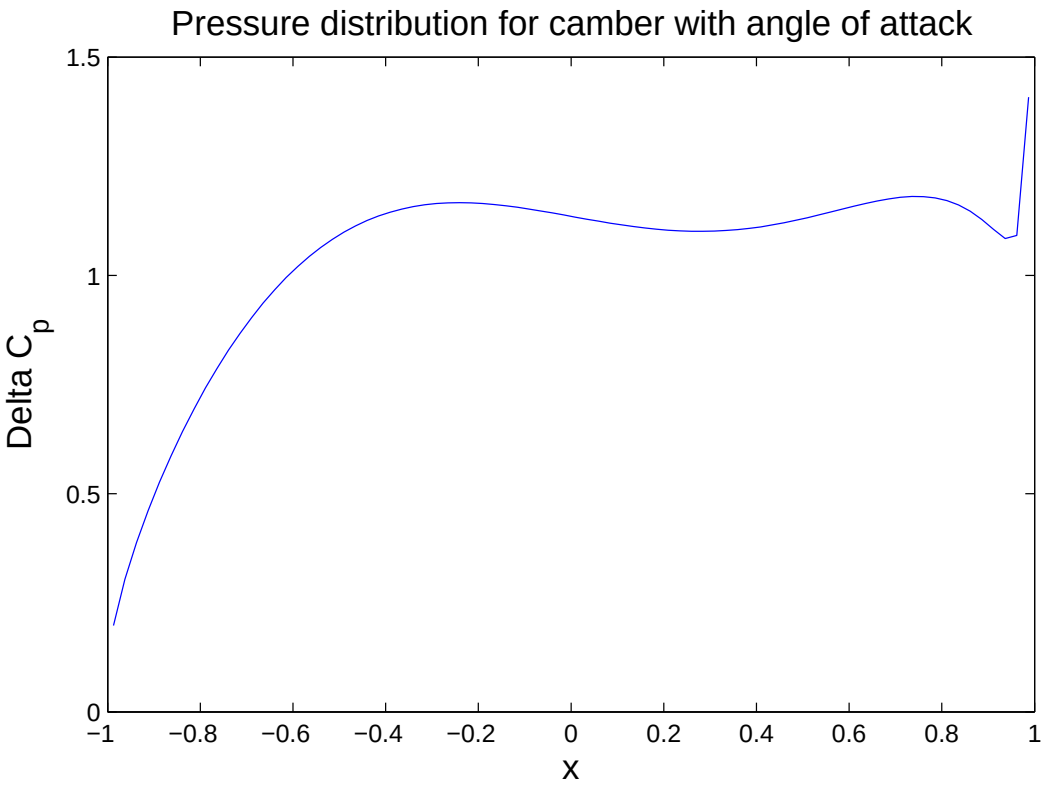

Figure 3.7: The pressure coefficient distribution, as seen in equation 2.15.

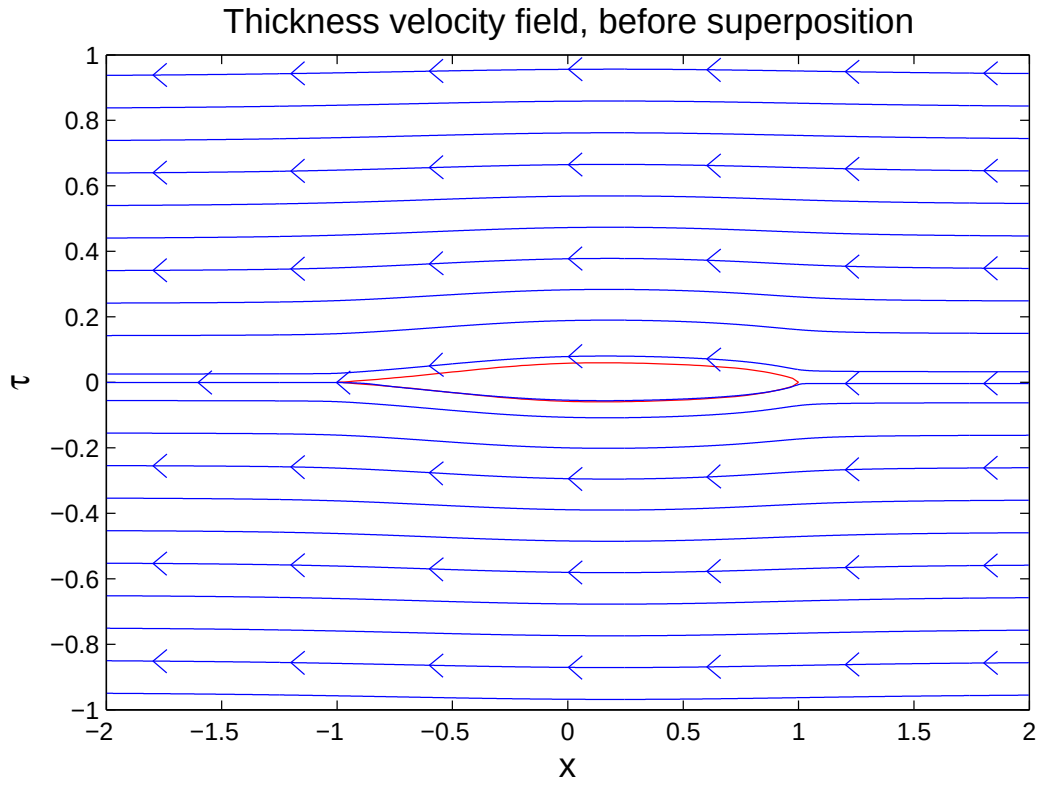

Figure 3.8: Plot showing the result of the thickness before superposition.

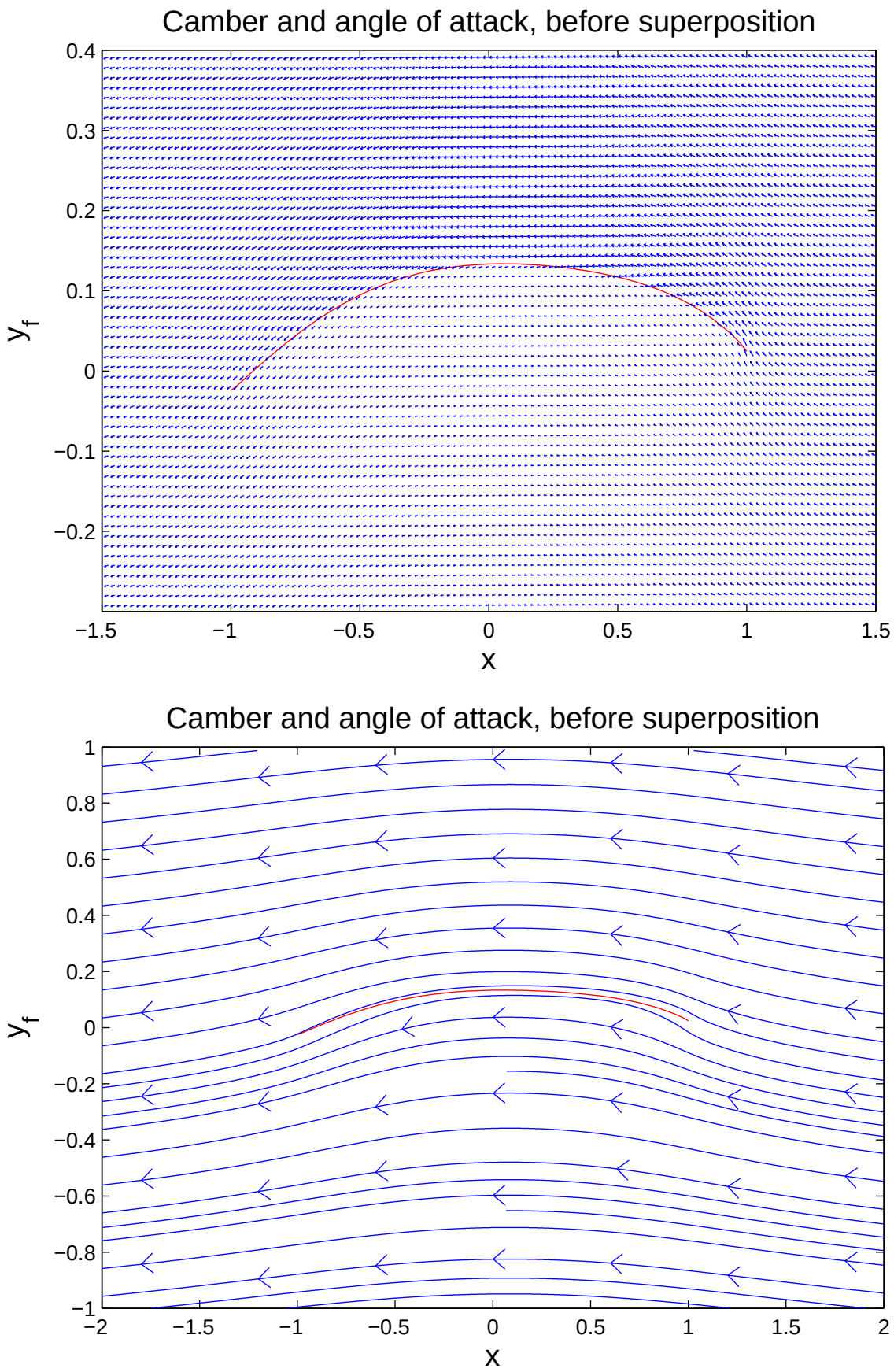

Figure 3.9: Plots showing the results of the camber before superposition.

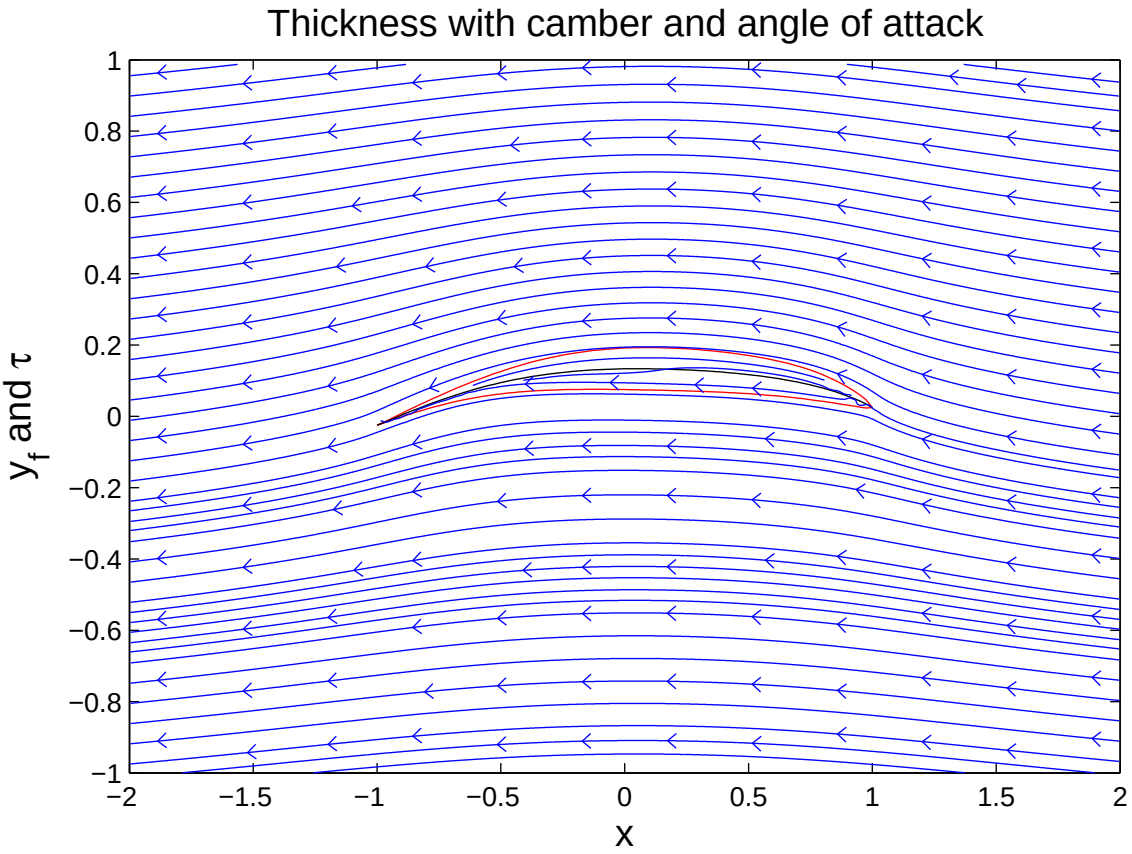

Figure 3.10: Plot showing the result of the superposition.

3.2 Assigned values

The Matlab script is used with the assigned values, as seen in table 3.1. The following were used:
a=1
U=1
dx=1.25
$\alpha = 1.4°$
$\beta = 0°$
b = 0

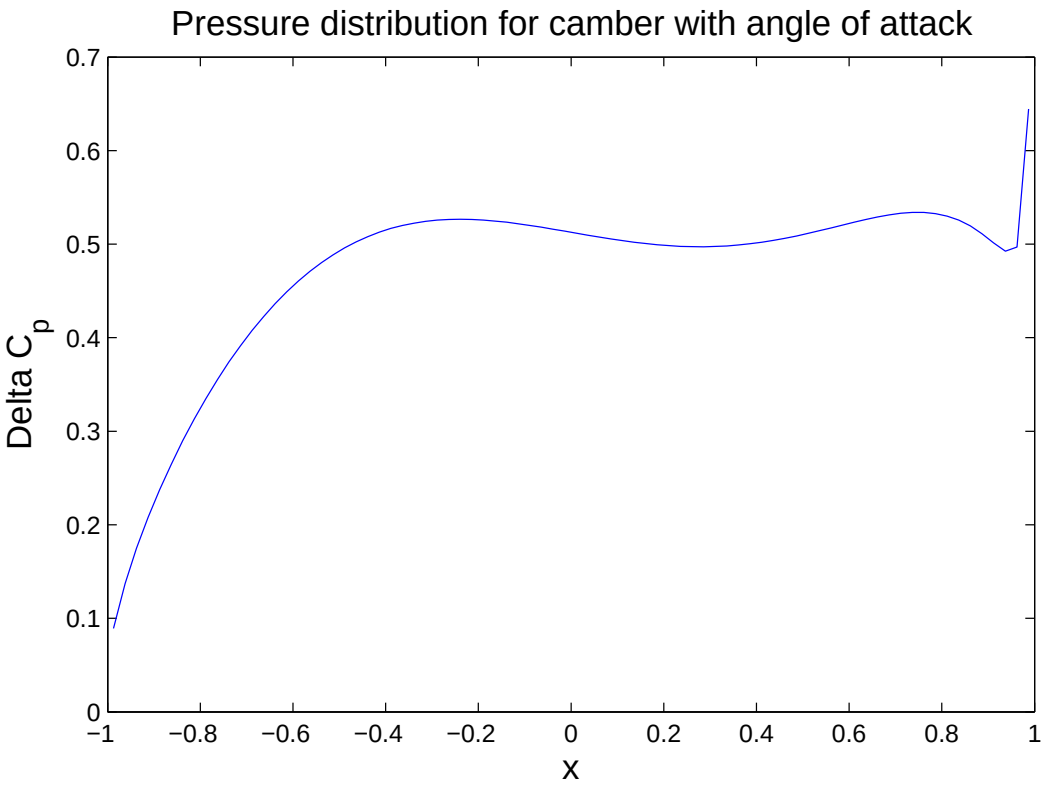

Figure 3.11: The pressure coefficient distribution, as seen in equation 2.15.

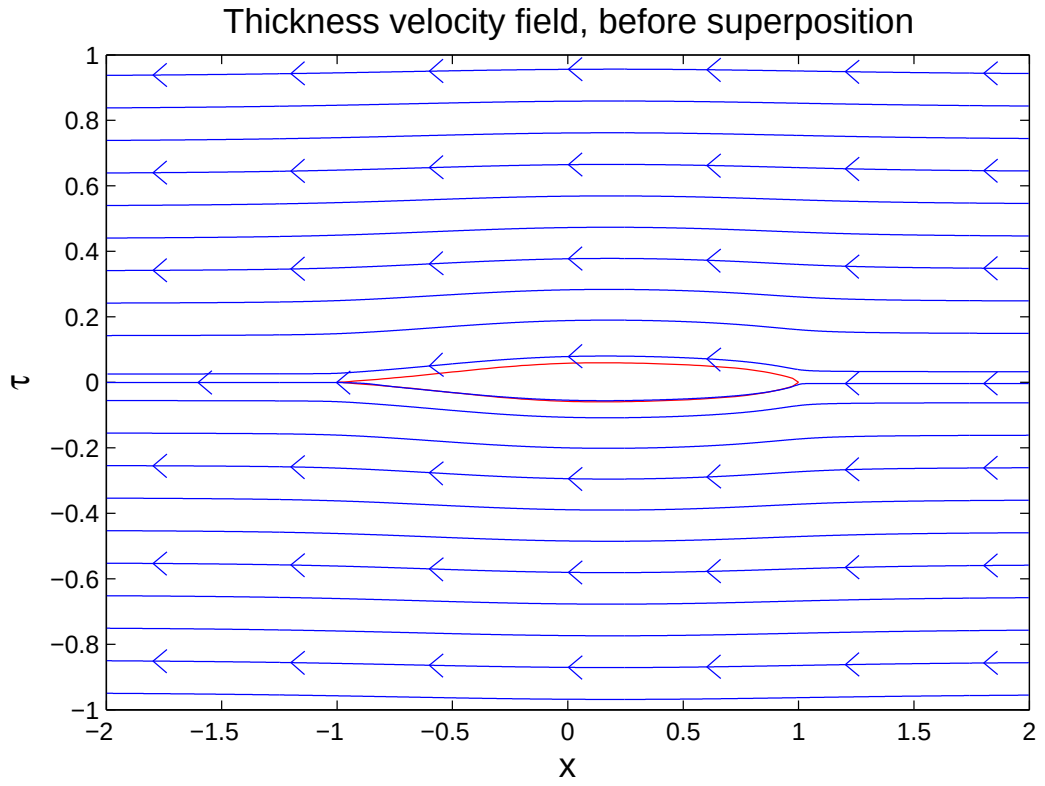

Figure 3.12: Plot showing the result of the thickness before superposition.

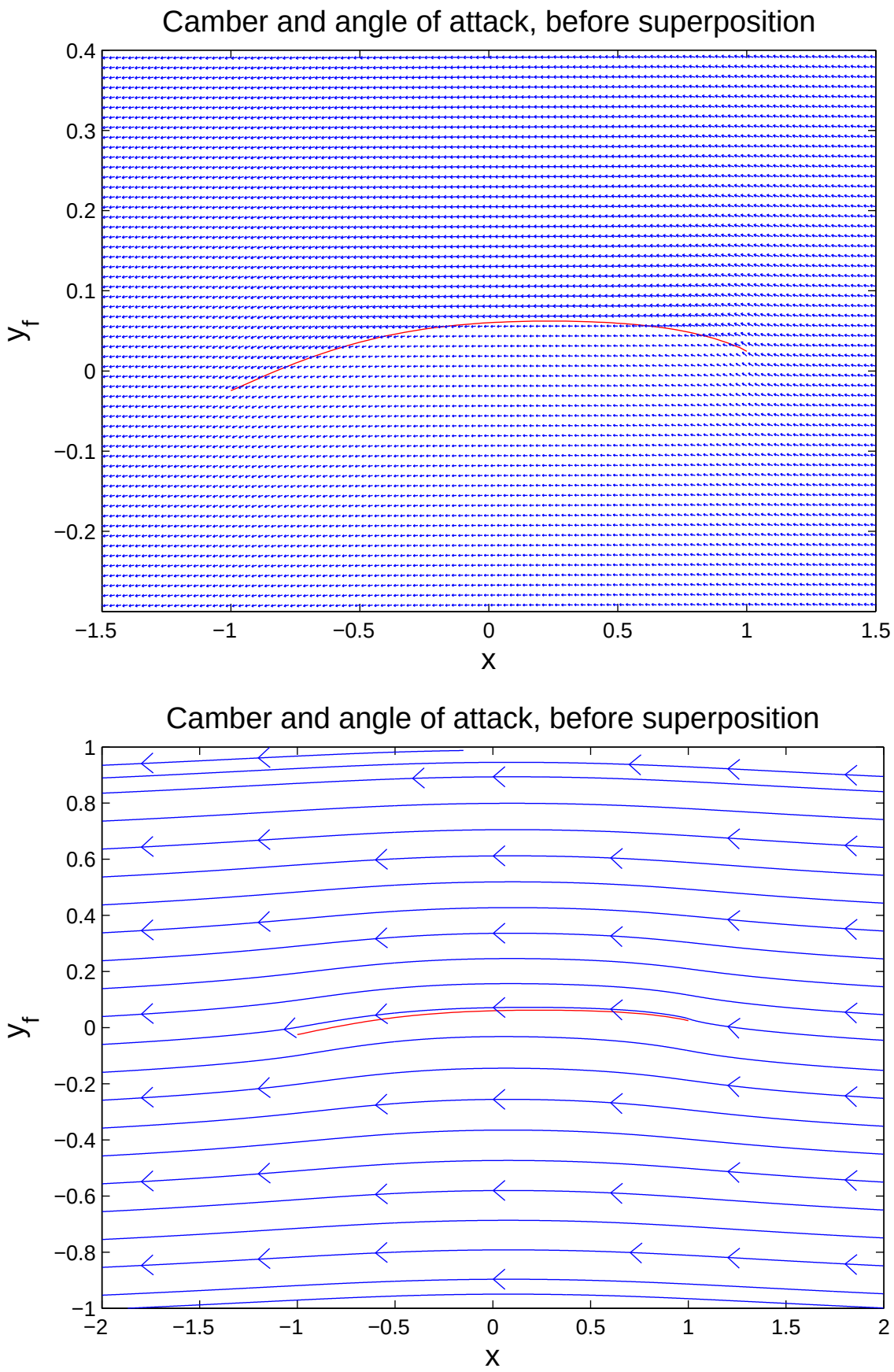

Figure 3.13: Plots showing the results of the camber before superposition.

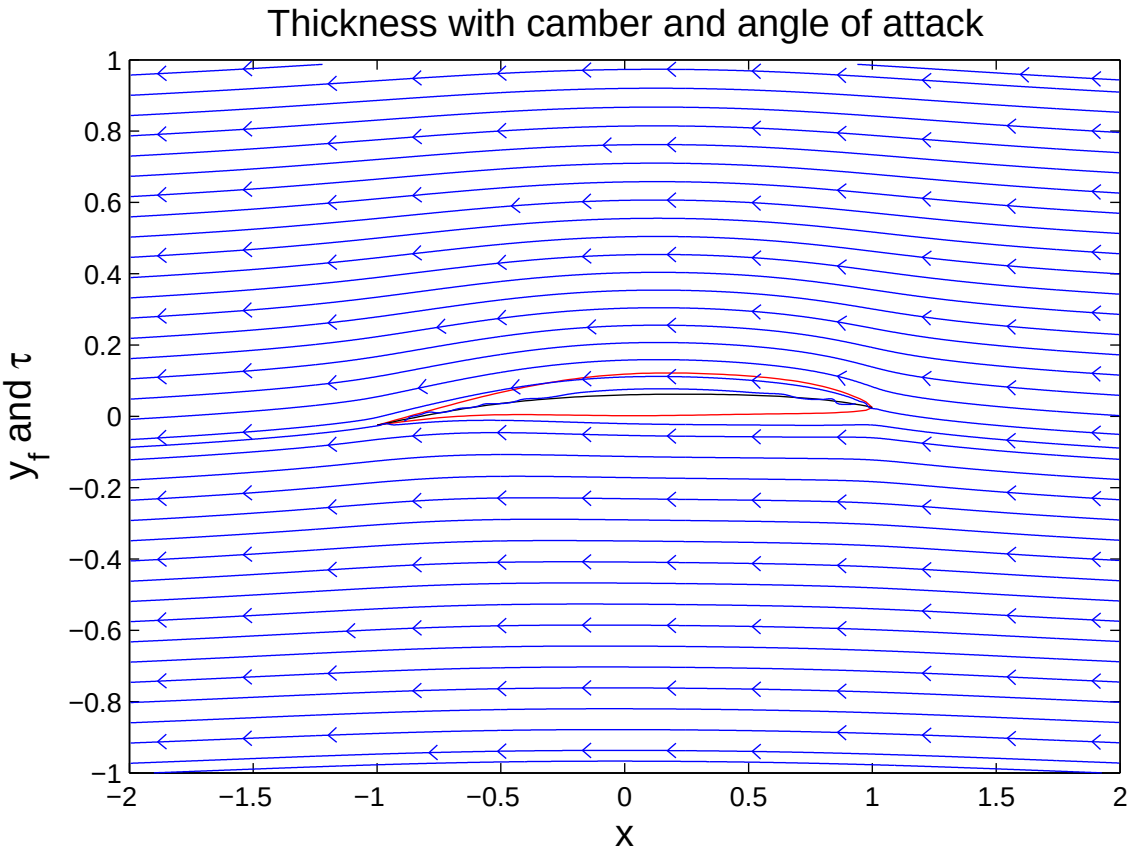

Figure 3.14: Plot showing the result of the superposition.

3.3 Overview of results from comparison

Results	NACA ideal values (book)	NACA ideal values	Assigned values
C_L	1.0	1.0422	0.4708
C_D		0.008811	0.008811

The pressure distributions, seen in figure 3.7 and 3.11 both have the same tendency. As they are made from the NACA **a**=0.8 profile, 80% of the pressure distribution is supposed to be linear. The reason for the deviations is due to the polynomiums used to model the camber, which smoothens out the curve. Furthermore the pressure at the leading edge is deviating a lot. As earlier described this happens because the induced velocity is equal to the onset velocity at the leading edge which does not fulfil the assumption that $u << U$.

The streamlines are clearly following the surface for both thicknesses in figure 3.8 and 3.12. It can be seen that the streamlines bend around the thickness of the section and also bends the flow lines in both vertical directions. After the foil the stream is uniform again. As the t/c values is the same for both situations nothing changes

between these two plots.

The cambers influence on the stream can be seen in figure 3.9 and 3.13. For both situations two plots are shown. The top one shows the direction of every single velocity within the field. Because of the resolution it can be hard to see, but the velocities are lower beneath the wing. This is because the streamlines going on top of the wing needs to accelerate relative to the streamlines going below, hence creating a lift. For the lower plot in each figure the streamlines are plotted. Here it is easier to see what happens. The streamlines follows the camber nicely and the effect of the camber can easily be seen on the flow.
In figure 3.10 and 3.14 the superposition can be seen. Most of the streamlines follows the foil as expected but some penetration of the foil can be seen. This might be due to inaccuracies of the plots or potentials. Otherwise the streamlines looks fine.

To investigate the accuracy of the script a comparison with the pressure distribution of the NACA mean line is made, see figure 3.15.

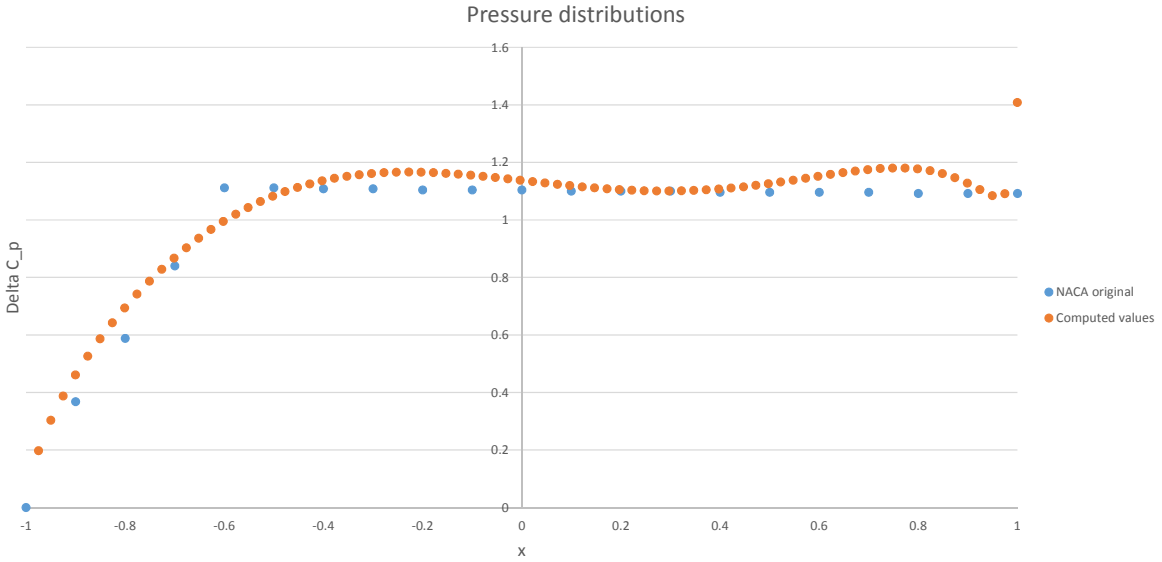

Figure 3.15: A comparison of the pressure coefficient distribution between the computed values and the actual NACA values

The difference is small and only the leading edge is deviating significantly as already discussed.
The deviation for the camber with angle of attack has been investigated. Now the deviations for the thickness will be looked into. The distributions of induced tangential velocities are plotted in figure 3.16 for y'=0 in equation 2.2.

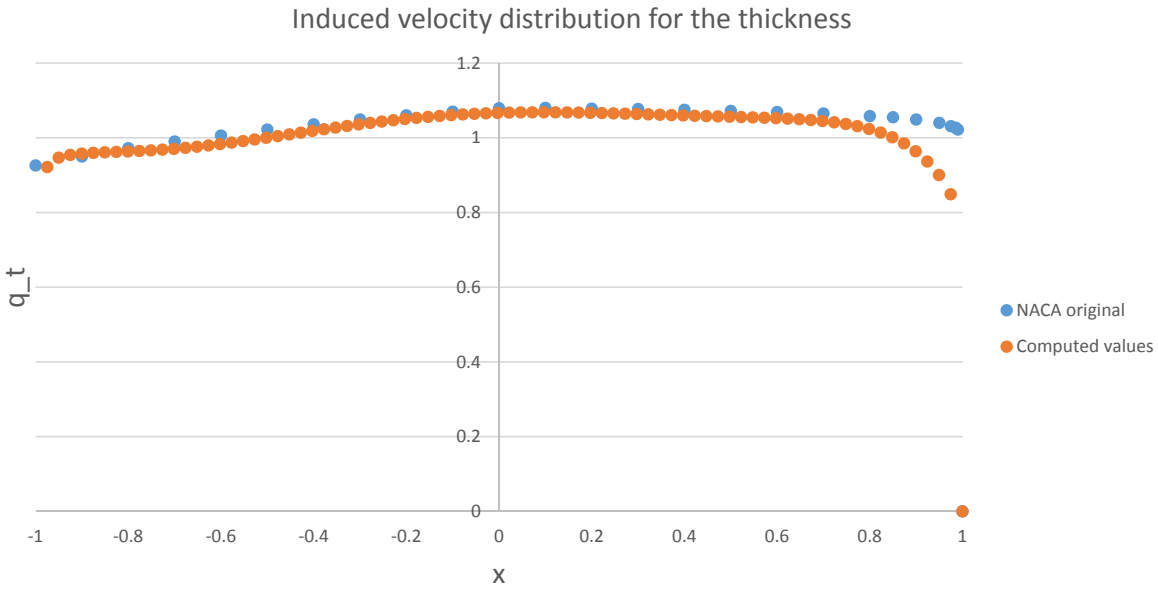

Figure 3.16: A comparison of the induced tangential velocity distribution between the computed values and the actual NACA values.

The velocity distributions are quite similar. The tendency is that the computed velocities are a little lower than the original values. Furthermore the leading edge experiences some deviations. This is probably due to some deviations in the theory at the leading edge.
Both the camber with angle of attack and the thickness have now been validated. They are both relatively close to the original NACA-values, and it is then assumed that the figures are valid.
The distribution of the strength of vortexes can be seen in figure 3.17.

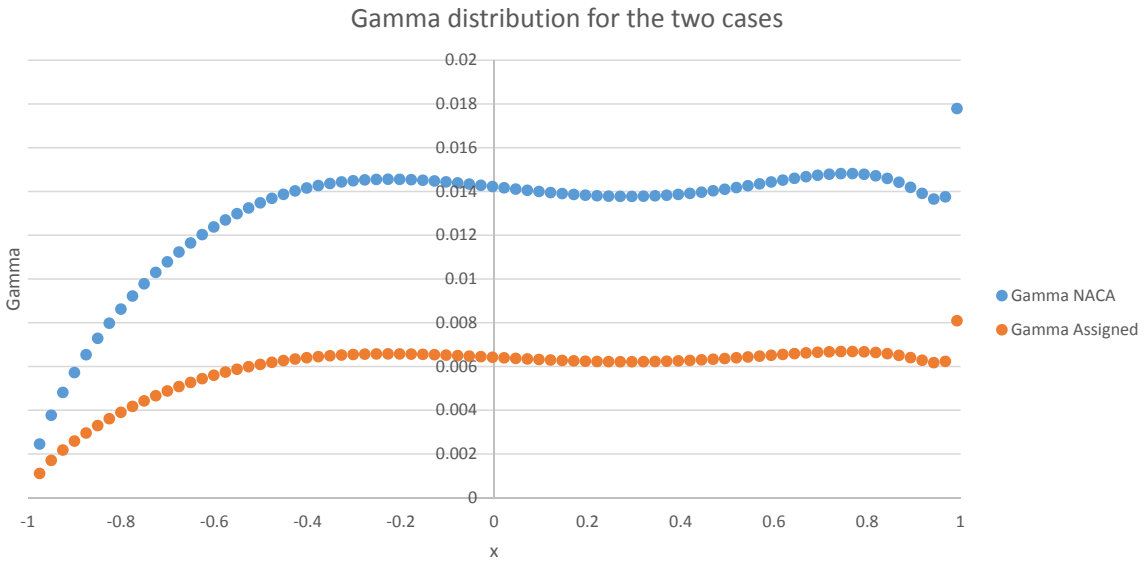

Figure 3.17: A comparison of the vortex strength, Gamma, for each case.

As expected the assigned values yields a lower value for Γ as the camber is smaller

hence making the lift lower. The overall tendency is the same for both, as we again see the polynomium fit dominating the expression. The leading edge vortex is, as in figure 3.15, deviating quite clear.

3.4 Drag and Flaps

The drag coefficient is found. As both foils have the same thickness, they also experience the same drag:

$$C_D = 0.00850 + 0.0864 \cdot 0.06^2 = 0.008811 \tag{3.24}$$

The drag is quite low but when compared to figure 7.13[1] the value is what you would expect from a NACA profile.

From "Exercise 3" in the course, the following conclusion was made for the use of flap with a flat plate:
Length of flap: $b = 1/4 * a$
Flap at TE: $C_{L_{flat}} = 2.768 \cdot \beta$
Flap at LE: $C_{L_{flat}} = 0.124 \cdot \beta$ Where β is the angle of the flap.

The lift of the flap is tested for:
$\beta = 20°$
Only the TE flap will be tested as it is the most effective. A flap at the LE will disrupt the flow, and reduce the velocities greatly, before going over the foil hence making it less effective.
The lift coefficient increase from the flap should be:

$$C_{L_{flap}} = 2.768 \cdot 20° \cdot \frac{\pi}{180} = 0.9662 \tag{3.25}$$

Running the script without flap and with no angle of attack yields the following lift:

$$C_L = 0.8937 \tag{3.26}$$

The expected lift with flap at an angle $\beta = 20°$:

$$C_{L_{total}} = 0.8937 + 0.9662 = 1.8599 \tag{3.27}$$

The actual lift coefficient from the script:

$$C_{L_{total}} = 1.7748 \tag{3.28}$$

There is a small deviation at about 5%, but the result is within reason especially considering that $C_{L_{flat}} = 2.768 \cdot \beta$ was found for a flat plate. The chamber without an angle of attack still achieves some lift, which will produce some error margin in the results.
Different configurations with flaps have been tested. The results can be seen in table 3.2.

	α=0, β=0,b=0	α=0, β=20°,b=$\frac{1}{4}$	α=1.4°, β=0,b=0	α=1.4°, β=20°,b=$\frac{1}{4}$
C_L	0.8937	1.7748	1.0440	1.9126

Table 3.2: Overview of results for different flap configurations with $\frac{f}{c} = 0.06651$ and $\frac{t}{c} = 0.06$

The results with flaps for zero angle of attack can be seen in figure 3.18 and 3.21.

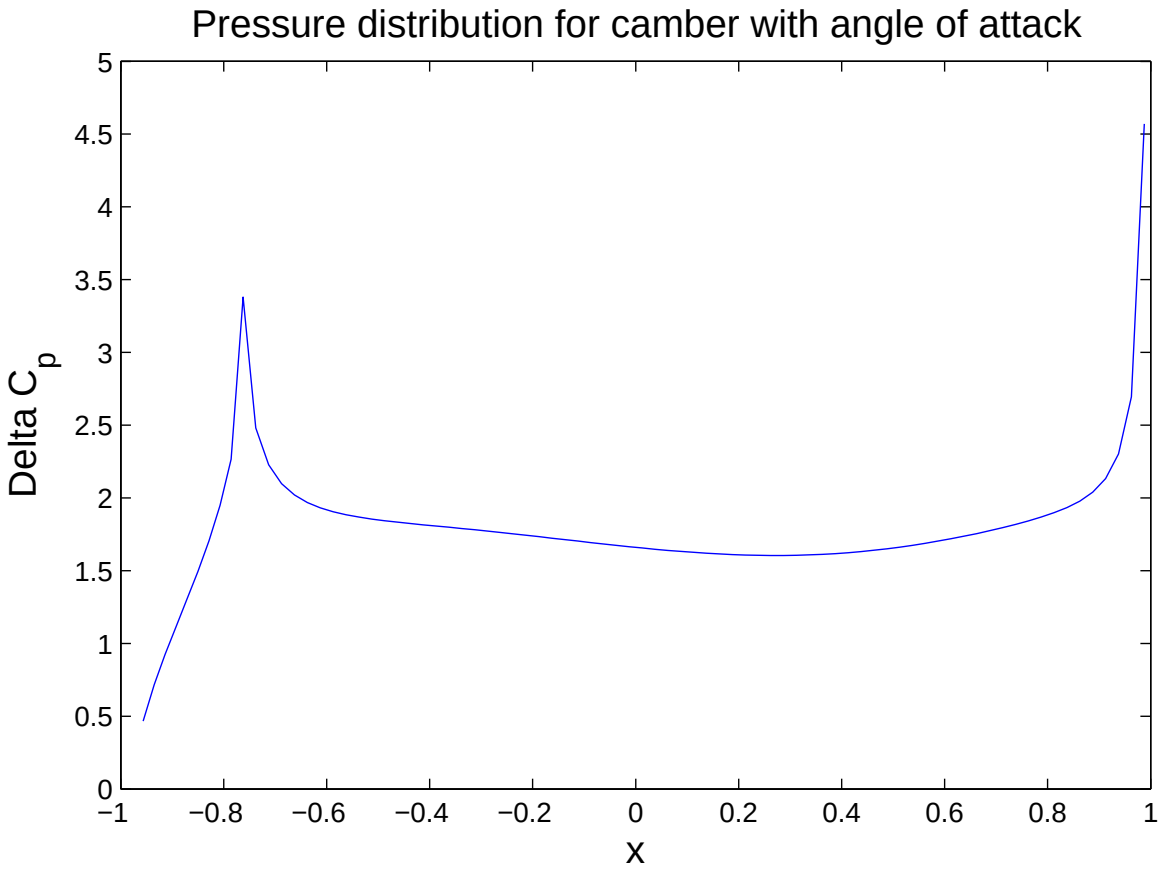

Figure 3.18: The ΔC_p pressure distribution with flaps for $\beta = 20°$, b = 1/4 and $\alpha = 0$.

As the lift increases in the camber, the pressure distribution also increases. b=1/4*a is equal to a distance of 0.25 on the x-axis, as a=1. From this it is clear that the new peak within the pressure distribution arises at the front of the flap. This happens because the velocity is slowed down when hitting the start of the flap. The whole pressure distribution is lifted and it is very clear that the flap has a great impact on the foil.
For comparison with the foil without the flap at zero angle of attack the pressure distribution can be seen in figure 3.19. First of all the overall pressure distribution is a lot smaller than with flaps, and secondly the leading edge pressure drops significantly.

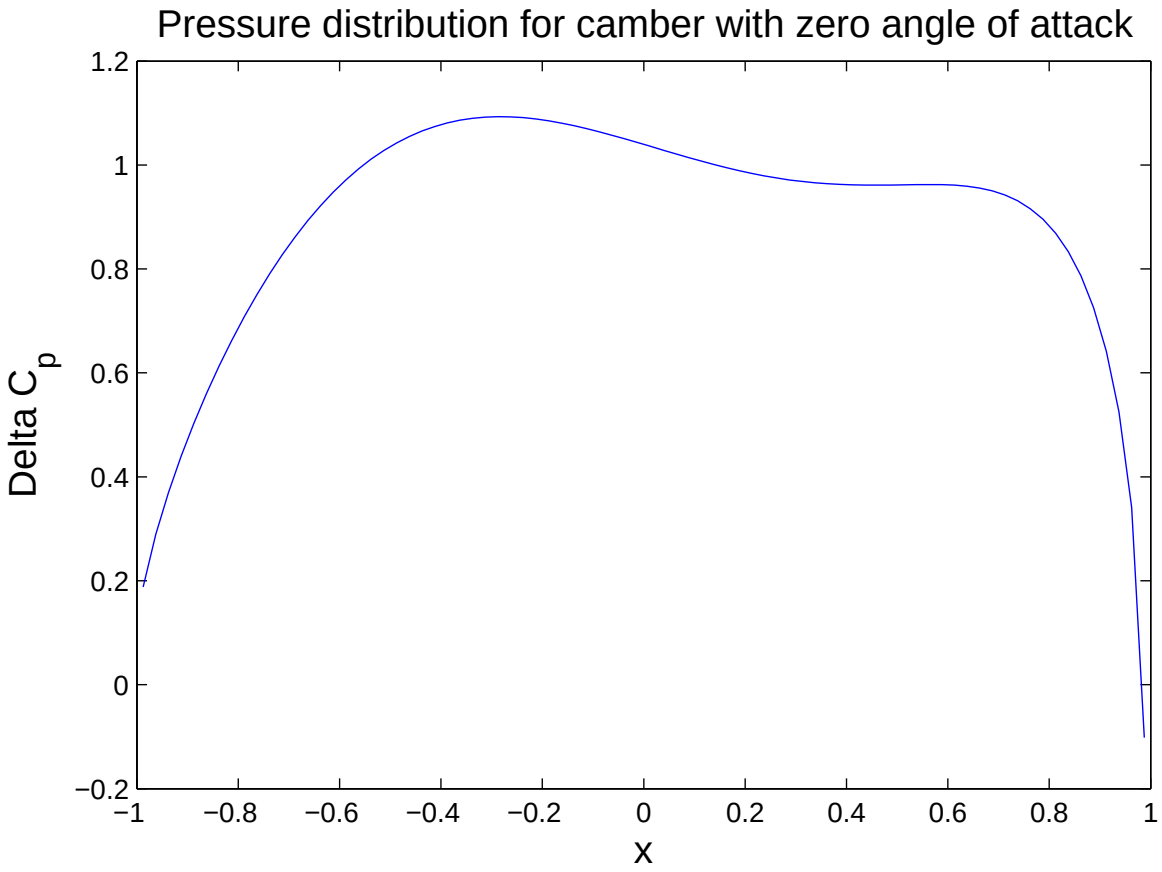

Figure 3.19: The ΔC_p pressure distribution without flaps, $\beta = 0°$, b = 0 and $\alpha = 0$.

In figure 3.21 the streamlines around the foil with the flap can be seen. It seems that some of the streamlines stops at the flap, which could mean that the velocity is decreased.

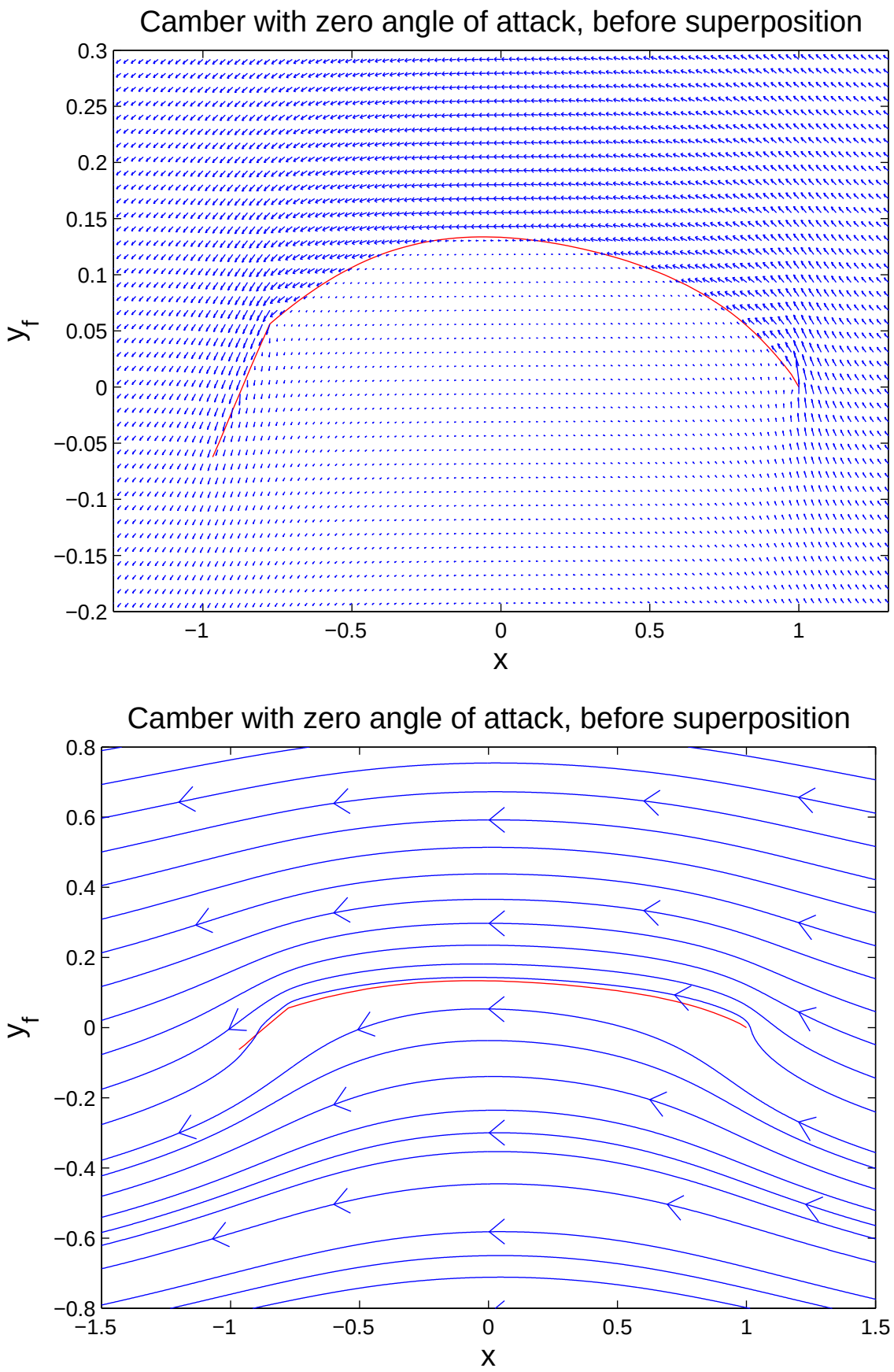

Figure 3.20: The camber with zero angle of attack and flaps for $\beta = 20°$, b = 1/4 and $\alpha = 0$.

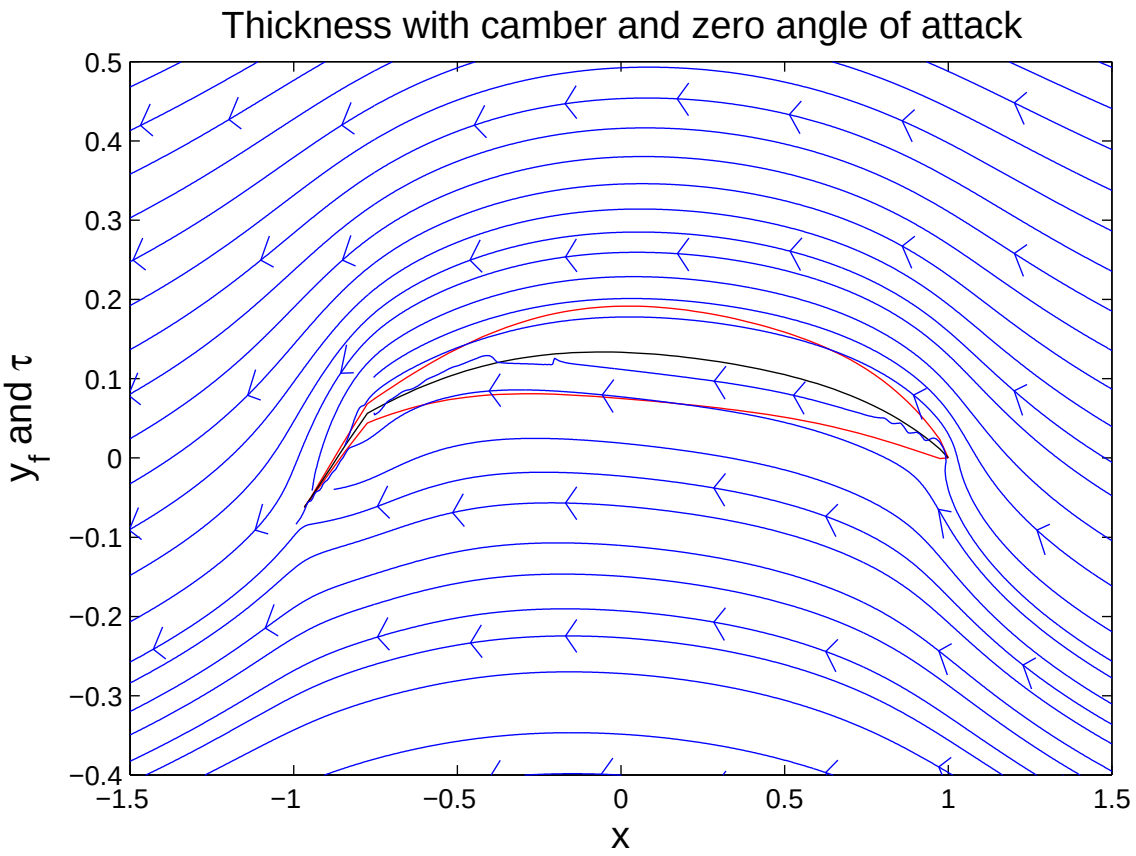

Figure 3.21: The foil with flaps for $\beta = 20°$, b $= 1/4$ and $\alpha = 0$.

As for the other plots showing the velocity fields, the streamlines follows the profile nicely and it is easily clear that the flaps interact with the flow. As before some penetration of the thickness occur but that is expected, as the potential theory is not exact.

References

[1] John P. Breslin, Poul Andersen, 1994, "Hydrodynamics of Ship Propellers", Cambridge Ocean Technology Series 3